INTERNATIONAL JOURNAL OF HYDROGEN ENERGY 40 (2015) 2890–2898

Available online at www.sciencedirect.com

ScienceDirect

journal homepage: www.elsevier.com/locate/he

A numerical investigation of structure and emissions of oxygen-enriched syngas flame in counter-flow configuration

Meriem Safer [a], *Fouzi Tabet* [b,*], *Ahmed Ouadha* [c], *Khadidja Safer* [a]

[a] *LCGE (Laboratoire des Carburants Gazeux et de l'Environnement), Faculté du Génie Mécanique, Université des Sciences et de la Technologie d'Oran Mohamed Boudiaf, BP 1505 Elmenaouar, Oran 31000, Algeria*

[b] *DBFZ (Deutsches Biomasseforschungszentrum gemeinnützige GmbH), Torgauer Straße 116, D-04347 Leipzig, Germany*

[c] *Laboratoire d'Energie et de Propulsion Navale, Faculté du Génie Mécanique, Université des Sciences et de la Technologie d'Oran Mohamed Boudiaf, BP 1505 Elmenaouar, Oran 31000, Algeria*

ARTICLE INFO

Article history:
Received 7 October 2014
Received in revised form
8 December 2014
Accepted 25 December 2014
Available online 17 January 2015

Keywords:
Syngas
Oxygen enrichment
NO_x emissions
Counter-flow diffusion flame
Flame structure

ABSTRACT

The aim of the present study is to investigate the enhancement of syngas combustion using the promising oxygen-enrichment technology, with a particular attention on optimal operating conditions in regard to NO_x emissions. For this purpose, a numerical study is conducted on a syngas counter-flow diffusion flame, using air enriched with oxygen as the oxidizer. The oxygen concentration ranges from 21% to 30% by volume. Two syngas compositions are considered with H_2/CO rates equal to 0.25 and 4, respectively. Flame structure is characterized by solving flamelet equations with the consideration of radiation. The chemical reaction mechanism used is GRI 3.0. Computational results showed that oxygen addition increases the flame temperature and intensifies the radiative heat transfer. It also considerably extends flammability limits allowing stable flames at high values of the scalar dissipation rates and for lean syngas composition. NO_x formation is substantially increased with oxygen increment, and Zeldovich mechanism is found to be the main route of NO_x formation. H_2-lean syngas flames produce less NO_x at low scalar dissipation while H_2-rich syngas flames NO_x emissions are low at high scalar dissipation rates.

Introduction

Conventional fuels are expected to be progressively replaced by cleaner energy sources, among which, hydrogen-rich fuels such as syngas, are due to become the most important alternative ones.

The use of syngas is of increasing interest, particularly for electricity production and as a component of the Integrated Gasification Combined Cycle concept (IGCC).

* *Corresponding author*. Tel.: +49 (0) 341 2434 495; fax: +49 (0) 341 2434 133.
E-mail addresses: safer.meriem@gmail.com (M. Safer), fouzi.tabet@dbfz.de (F. Tabet), ah_ouadha@yahoo.fr (A. Ouadha), khsafer@gmail.com (K. Safer).

http://dx.doi.org/10.1016/j.ijhydene.2014.12.117

The composition of syngas is strongly dependent on the fuel source and processing technique [1]. Syngas may have wide variations of H_2/CO ratios. Hence, combustion properties such as flammability limits and flame temperature will be accordingly variable. In addition, syngas, as many alternative fuels, has lower calorific value than conventional fuels such as methane. According to McLean et al. [2], a syngas with a H_2/CO ratio equal to 0.5 has a Low Heating Value (LHV) of 10.5 MJ/kg, while methane has a LHV of 50 MJ/kg [3].

Oxygen-Enriched Combustion (OEC) has been advanced as cost effective option to improve combustion process (stability and reactivity) [4]. Oxygen-enriched combustion, also known as oxygen-enhanced combustion, uses oxidizers with oxygen concentrations higher than that in air (21% by volume). It is applied since many years, in different industries, such as cement and glass factories, waste incineration and steel smelting. OEC has received, by the past, little attention from the academic combustion community, due to safety considerations and high costs of oxygen production [4]. Recent investigations showed that increasing oxygen concentration in the oxidizer induces several benefits including higher flame temperatures, rising productivity and significant reduction in fuel consumption [5,6]. Moreover, recent increasingly strict emissions regulations and costs reduction of oxygen production have revived the interest of researchers to oxygen-enhanced combustion.

Tan et al. [7] carried out an experimental study on the effects of oxygen enrichment in air and CO_2 atmospheres in the case of methane flame using a vertical combustor. The O_2 concentration was set to 28% in both cases. Very high levels of NO_x were obtained in O_2 enriched air combustion due to higher flame temperatures while nearly no NO_x emissions were observed in O_2/CO_2 combustion due to the absence of N_2 in the feed air. Cheng et al. [8] investigated by both numerical simulation and optical measurements the structure of a planar oxygen-enriched methane counter-flow flame. They particularly focused their attention on the effects of stretch and oxidizer oxygen concentration. They found that, for a given value of stretch, flame temperature increased significantly with oxygen concentration. Moreover, they observed that oxygen enrichment considerably enhanced extinction limits. Chen and Axelbaum RL [9] conducted an experimental and a numerical study to examine the effects of oxygen-enrichment and fuel dilution on flame extinction. They considered a counter-flow flame configuration and four different fuels: methane, ethane, ethylene and propane. The range of oxygen mass fraction variation was from 0.233 to 1.0. Results indicated that an appropriate adjustment of oxidizer oxygen and fuel concentrations give improved extinction characteristics. In other words, an optimal oxygen-enrichment, combined with fuel dilution, leads to strong flames [9]. A numerical study of CH_4/air and CH_4/O_2 counter-flow laminar flames was performed by Urzica and Gutheil [10] using a detailed chemical reaction mechanism. The laminar CH_4/O_2 flame was studied under pressures ranging from 0.1 MPa to 2 MPa. It was shown that maximum flame temperature increased significantly with oxygen concentration in the oxidizer. The same trend was observed for radicals CO, O and OH. Furthermore, comparison between CH_4/air and CH_4/O_2 flames at strain rate near extinction revealed that flame thickness decreased considerably when oxygen oxidizer content increased. Global effects of oxygen-enhancement on radiative heat flux characteristics of methane non-premixed oxyfuel flames were examined experimentally by Ditaranto and Oppelt [11]. The oxidizer oxygen concentrations were varied from 35% to 70%, and CO_2 was used as a diluent. The measurements performed along the flame axis showed that the distribution of radiative heat flux and the flame length became shorter when the oxygen concentration increased. Moreover, the peak of radiated heat flux increased with oxygen concentration [11]. Furthermore, the intensity of visible spectra of these flames was more important with oxygen enrichment. Joo et al. [12] performed a numerical and an experimental study of the structures of laminar diffusion methane/oxygen and methane/air flames under a wide range of operating pressures (from 1 atm to 60 atm). The authors observed that, as the pressure increased, the visible flame height of the methane/oxygen flames decreased, while the visible flame height of methane/air flames remained constant. The comparison of soot production, for different pressures, showed that maximum soot fraction produced by methane/air flames was considerably higher than in methane/oxygen flames [12].

Yepes et al. [13] analyzed experimentally and numerically the laminar burning velocities of a syngas mixture containing 20% H_2, 20% CO and 60% N_2 using oxygen enriched air with enrichment levels varying from 21% to 35% by volume. They found that oxygen rise in the combustion air increased the laminar burning velocity of the syngas mixture, leading to an intensification of the reaction rate.

The literature on oxygen-enhanced diffusion flames is abundant, but only few studies are devoted to syngas oxygen-enhanced flames characteristics.

The aim of this study is to examine numerically the impact of oxygen enrichment on the structure and emissions of syngas flame in counter-flow configuration. The calculations are conducted over a large range of scalar dissipation rates (from near equilibrium to near extinction) for oxygen concentration ranging from 21% to 30% by volume, and for two

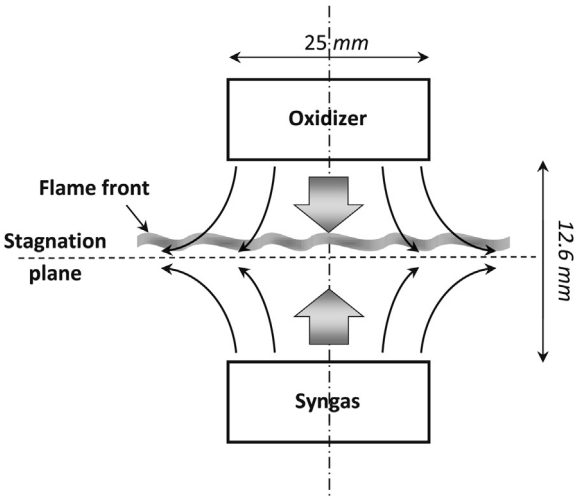

Fig. 1 – Flame configuration.

syngas compositions (H_2/CO ratio = 0.25 and 4.0). Special focus is paid to NO_x emissions.

The article consists of four sections. Following a brief explanation of the modeling approach, a general description of the simulation details is introduced. The numerical simulation results are then presented with a discussion in the last section. The conclusion summarizes the findings of the present work.

Calculation methodology

The flame configuration considered in the present work is described in Fig. 1. It is a counter-flow, laminar diffusion flame, stabilized near the stagnation plane of two opposing fuel and oxidant jet flows.

A one dimensional description of the local flame structure in mixture fraction space is given by flamelet equations with the scalar dissipation rate as a free parameter. Flamelet approach assumes a one-dimensional behavior of the combustion phenomena in the normal direction to the flame front. Flamelet equations are derived from energy and species transport equations by applying a coordinate transformation [14]. In these equations, temperature and species mass fractions are function of a conserved scalar known as mixture fraction Z. In addition, a parameter called scalar dissipation rate χ totally represents the influence of the flow field on the flamelet structure:

$$\rho\frac{\partial Y_n}{\partial t}=\frac{1}{2}\rho\chi\frac{1}{Le_n}\frac{\partial^2 Y_n}{\partial Z^2}+\dot{\omega}_n-\frac{1}{2}\frac{\partial Y_n}{\partial Z}\left[\frac{1}{2}\left(1-\frac{1}{Le_n}\right)\left(\frac{\partial\rho\chi}{\partial Z}+\rho\chi\frac{C_p}{\lambda}\frac{\partial\left(\frac{\lambda}{C_p}\right)}{\partial Z}\right)\right] \tag{1}$$

$$\rho\frac{\partial T}{\partial t}=\frac{1}{2}\rho\chi\frac{\partial^2 T}{\partial Z^2}-\frac{1}{C_p}\sum_n H_n\dot{\omega}_n+\frac{1}{2c_p}\rho\chi\left[\frac{\partial C_p}{\partial Z}+\sum_n\frac{1}{Le_n}c_{p,n}\frac{\partial Y_n}{\partial Z}\right]\frac{\partial T}{\partial Z}-\frac{1}{C_p}\left[4\sigma p\sum_i X_i a_n\left(T^4-T_b^4\right)\right] \tag{2}$$

The notation in Equations (1) and (2) is as follows: Y_n, T, ρ are the nth species mass fraction, mixture temperature and density, respectively. Le_n is the Lewis number of the nth species defined as $Le = \lambda/(\rho D_{nm} C_p)$ where D_{nm} is the multi-component ordinary diffusion coefficient, $\dot{\omega}_n$ is the nth species reaction rate and χ is the instantaneous scalar dissipation rate defined by: $\chi = 2D_z(\nabla Z\cdot\nabla Z)$. Its modelling is based on the relation below which is taken from the counter-flow geometry [15]:

$$\chi=\chi_{st}\frac{\phi}{\phi_{st}}\frac{g(Z)}{g(Z_{st})} \tag{3}$$

χ_{st} is the scalar dissipation rate at stoichiometry and ϕ is a factor introduced in order to include the effect of density variation [15]:

$$\phi=\frac{1}{4}\frac{3\left(\sqrt{\rho_\infty/\rho}+1\right)^2}{2\sqrt{\rho_\infty/\rho}+1} \tag{4}$$

The subscript ∞ means the oxidizer stream. The function $g(Z)$ is given as follows [15]:

$$g(Z)=\exp\left[-2\left(erfc^{-1}(2Z)\right)^2\right] \tag{5}$$

where $erfc^{-1}$ is the inverse of the complementary error function.

The last term in Equation (2) is an optically thin model for radiative energy loss from the flamelet. Here, σ is the Stefan–Boltzmann constant, P is the pressure, X_n is the nth species mole fraction, a_i are polynomial coefficients for the Planck mean absorption coefficients [16] and T_b is the far-field (background) temperature. Radiative gaseous species considered are CO, CO_2 and H_2O.

The validity of the optically model for hydrogen and hydrogen enriched flames (H_2/He, CO/H_2/N_2, CH_4/H_2/N_2) was, previously, confirmed by Barlow et al. [16] and Frank et al. [17]. In addition, many authors calculated syngas flames using optically thin model (Som et al. [18], Park et al. [19], Kim et al. [20]).

The two input parameters in Equations (1) and (2) are mixture fraction Z and stoichiometric scalar dissipation rate χ_{st}.

Simulation details

Flamelet Equations (1) and (2) are solved from near equilibrium to near extinction until steady state is achieved assuming $Le_n = 1$ for all the species involved in the chemical mechanism using the PrePDF 4.0 code [21]. Computations are performed for two syngas compositions (lean and rich syngas) using five levels of O_2 in the oxidizer. A total of ten computations is carried out (Table 1). The operating pressure is maintained at 1 atm.

The assumption regarding the Lewis number is reasonable in this flame conditions. Differential diffusion was found to play a significant role in diluted and non-diluted syngas flames with high H_2 content in the fuel (>80%) at small strain rates (near equilibrium) (Park et al. [19]; Drake and Blint [22]; Park et al. [23]).

Syngas oxidation chemistry is modeled using GRI 3.0 mechanism [24] that involves 53 species and 325 reactions. The oxidation chemistries of CO and H_2 which are the dominant components of most syngas fuels are well represented in

Table 1 – Flame parameters.

H_2/CO	O_2 volume fraction (%)	Scalar dissipation rates (s^{-1})
0.25	21	From 0.1 to 5000
	23	
	25	
	27	
	30	
4.0	21	From 0.1 to 5000
	23	
	25	
	27	
	30	

this mechanism. GRI 3.0 mechanism was used in many previous studies of syngas counter-flow flames (Park et al. [25], Shih et al., [26]). Its accuracy was also assessed in the case of syngas in both air combustion and oxygen-enhanced combustion employing experimental data and predictions of existing syngas kinetics namely Davis et al. [27] mechanism, San Diego (Petrova and Williams [28]) mechanism and (Mueller et al. [29]) mechanism on laminar burning velocity where reasonable agreement was achieved (Yepes and Amell [13]; Som et al., [18]; Singh et al., [30]).

In addition, the study of Sahu and Ravikrishna [31] in which five chemical kinetic mechanisms namely, H_2/CO mechanism by Davis et al. [27], C1 mechanism from Li et al. [32], full chemistry from Li et al. [32], H_2/CO mechanism by Ranzi et al. [33] and GRI 3.0 [24] were compared to predict NO_x routes in syngas flames highlighted the importance of GRI 3.0 mechanism for prompt NO calculation.

Results and discussion

Model validation

The accuracy of flamelet model was demonstrated in previous study [14,15] where it was shown that flame structure is sufficiently well described. Further validation of this model is conducted here in the case of oxygen-enhancement combustion employing the experimental data of Cheng et al. [34] which corresponds to methane as no measurements of syngas combustion with enriched air in counter-flow diffusion flame configuration are currently available. The experimental device in Ref. [34] is an opposed-jet burner formed by two axisymmetric nozzles of 25 mm diameter, separated by a distance of 12.6 mm. The design of this burner was based on the study of Seshadri et al. [35]. The fuel was a mixture of nitrogen and methane and the oxidizer was oxygen at different concentrations ranging from 23% to 100% by volume. The ambient pressure was set to 1 atm. Measurements of the species concentration were made along the centerline of the burner using the nonintrusive Raman diagnostic system. The local flame temperature was determined from the species concentration using the ideal gas law. Fig. 2 shows a comparison between predictions and experiments for peak temperature variations with oxygen concentration at scalar dissipation rate value of 60 s^{-1} and methane concentration of 20% by volume. Very good agreement is obtained at this flame conditions.

Fig. 3 illustrates a comparison between predictions and experiments for peak temperature variations with methane concentration. In this case, oxidizer was pure oxygen and the scalar dissipation rate was 60 s^{-1}. Here again, both experimental and numerical results match well. Moreover, the results show similar extinction limit which is reached at 8% methane by volume.

Effect of scalar dissipation rate and fuel composition on maximum flame temperatures

Fig. 4 shows the maximum flame temperatures, as a function of scalar dissipation rate with and without the consideration of flame radiation, for both H_2-lean (Fig. 4a) and H_2-rich (Fig. 4b) syngas composition, respectively. Oxidizer is air, inlet temperature is 300 K and ambient pressure is 1 atm. It can be seen that without radiation, the maximum adiabatic flame temperature has a monotonic trend, for both compositions. It decreases with increasing scalar dissipation rate, until extinction. The adiabatic flame is blown off because very high scalar dissipation rates cause very short species residence times in the flame zone and lead to incomplete reactions. However, with thermal radiation, the maximum flame temperature exhibits a peak at an intermediate scalar dissipation rate ($\chi \approx 5.0$ s^{-1} for H_2-rich composition and $\chi \approx 25.0$ s^{-1} for H_2-lean composition). This result is different to the case without radiation, and this difference grows to be very large as scalar dissipation rate decreases. At low scalar dissipation rates, the flame temperature drops significantly because radiation heat losses increase, which results in a lower reaction

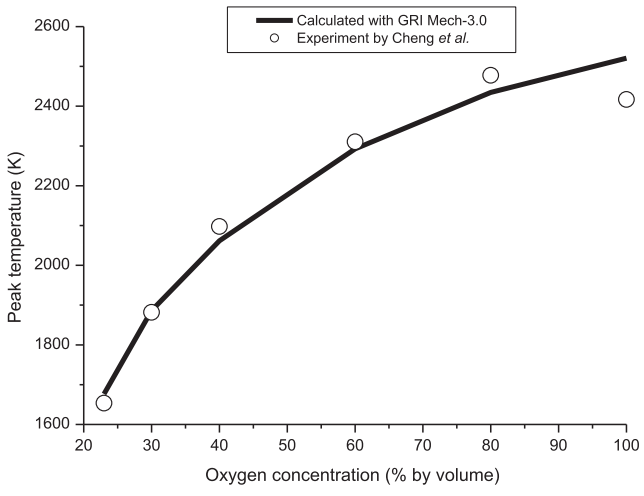

Fig. 2 – Comparison between predictions and experimental results of Cheng et al. [34]: peak flame variations with oxygen variations.

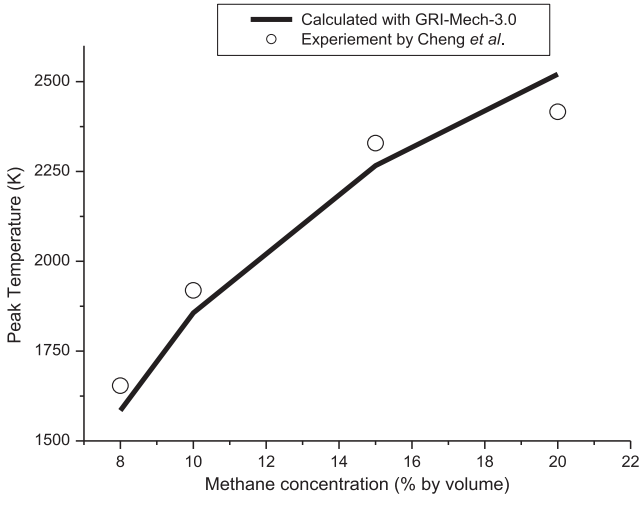

Fig. 3 – Comparison between predictions and experimental results of Cheng et al. [34]: peak flame variations with methane variations.

rate and higher reactants leakage [36]. The flame extinction occurs at high stretch rate due to insufficient gas residence time for chemical reactions. Radiative heat loss is mainly dependent on upon flame volume and the thickness of reaction zone is relevant to the reciprocal of scalar dissipation rate. Consequently, the difference of maximum flame temperatures with and without radiation becomes small with the increase of scalar dissipation rate. This general trend has been identified in previous studies [37,38]. In addition, radiation is found to be important only at strain rates lower than the intermediate value [37] and its effect decreases with hydrogen enrichment [39].

Effect of oxygen-enrichment on flame structure and NO emissions

In this section, the effect of oxygen-enrichment on temperature, flame structure and NO emissions is examined. Figs. 5 and 6 illustrate the profiles of temperature and species for oxygen concentrations ranging from 21% to 30% by volume for two syngas compositions ($H_2/CO = 4.0$ and $H_2/CO = 0.25$). Ambient temperature and pressure considered are 300 K and 1 atm, respectively. The scalar dissipation rate is 10 s^{-1}. From Fig. 5, oxygen addition in the oxidizer induces a significant increase of flame temperature. Indeed, for hydrogen rich composition, temperature rises by 18% when oxygen concentration increases from 21% to 30% (by volume) while the increase is about 10% for hydrogen lean case. Oxygen-enrichment implies less nitrogen in the oxidizer; therefore, the flame dilution is low in comparison to air combustion. Then, heat losses in flue gases diminish and less fuel is needed to maintain a given temperature. This finding signifies that O_2 addition in industrial combustion devices involves an important fuel saving [40]. Moreover, oxygen addition in the oxidizer induces a slight shift of the maximum flame temperature towards the fuel side together with a reduction of the flame zone.

From Fig. 6, oxygen enrichment has an important influence on the syngas combustion kinetics. Oxygen concentration increment intensifies species production such as H_2O (Fig. 6a), CO_2 (Fig. 6b), OH (Fig. 6c) and O (Fig. 6d). Fig. 6b indicates that oxygen rise promotes CO_2 formation. Indeed, for $H_2/CO = 4.0$ (i.e. rich syngas composition), CO_2 increases by 34% between 21% and 30% of oxygen concentration, while it increases by 27% for $H_2/CO = 0.25$ (i.e. lean syngas composition). This feature can be profitably exploited in industry to improve CO_2 capture in the flue gas [41].

Flame fractional temperature is introduced to characterize flame radiation as follows [25]:

$$f = \frac{T_{nonrad} - T_{rad}}{T_{nonrad}} \quad (6)$$

In this equation, T_{rad} is the flame temperature with the inclusion of radiative heat flux and T_{nonrad} is the flame temperature without radiative heat flux.

From Fig. 7, the fractional flame temperature at a fixed scalar dissipation rate of 10 s^{-1} increases with oxygen enhancement. This is mainly related to carbon dioxide production increase. Carbon dioxide being a strong gas radiation source. Oxygen addition intensifies radiative heat transfer of the syngas flame. This finding is concordant with the experimental observations of Wu et al. [40]. Furthermore, the effect

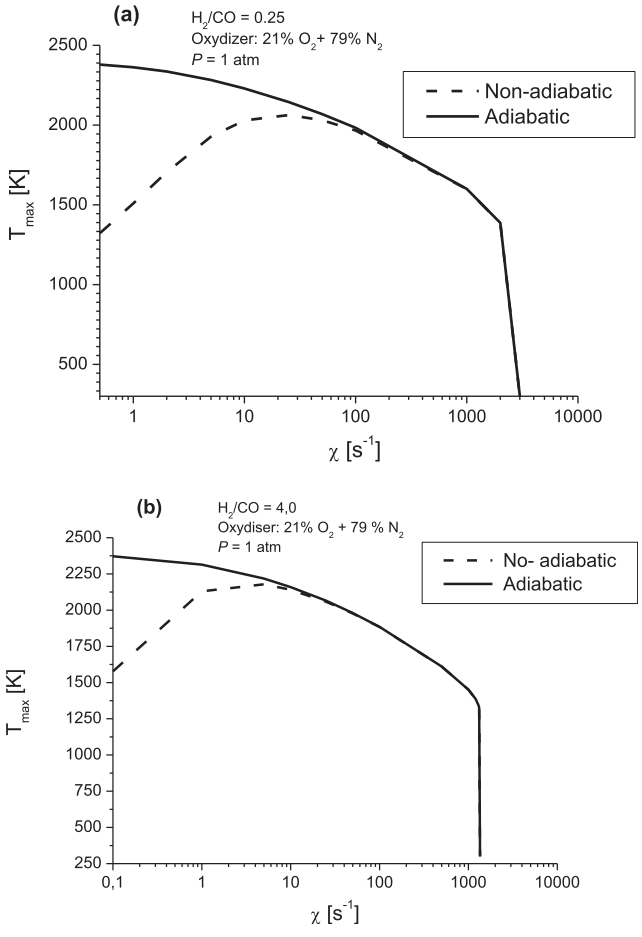

Fig. 4 – Maximum flame temperature variations with dissipation rate, with and without the consideration of flame radiation: (a) lean syngas composition case (b) rich syngas composition case.

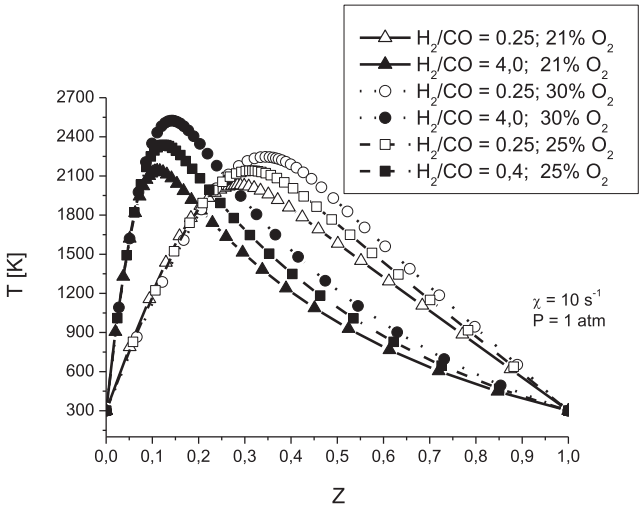

Fig. 5 – Effects of oxygen enrichment on temperature profiles (1 atm, 300 K, $\chi = 10\ s^{-1}$) for rich and lean syngas.

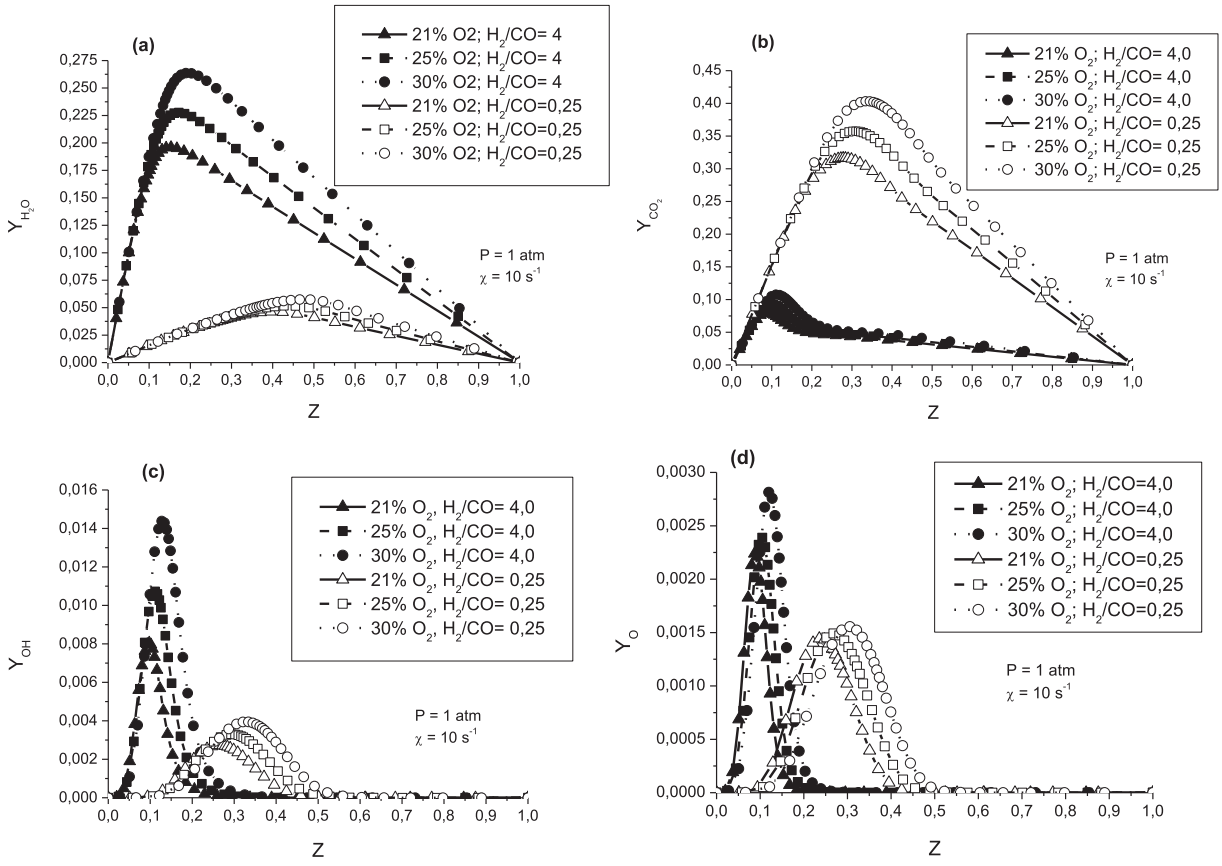

Fig. 6 – Effects of oxygen enrichment on flame structure (1 atm, 300 K, $\chi = 10\ s^{-1}$) for rich and lean syngas: profiles of (a) H_2O, (b) CO_2, (c) OH and, (d) O.

of oxygen increment on the fractional flame temperature is amplified by the increase of CO mole fraction in synthetic gas mixture as CO and CO_2 are very radiative species [25].

Fig. 8 depicts the variations of maximum flame temperature with scalar dissipation rate, for different oxygen concentrations. Flame temperature increases from a minimum value, which corresponds to the quenching limit, up to a peak, and then drops with scalar dissipation rate increase until blow-off. For low scalar dissipation rates, radiative losses prevail, so the temperature is too low to sustain the flame,

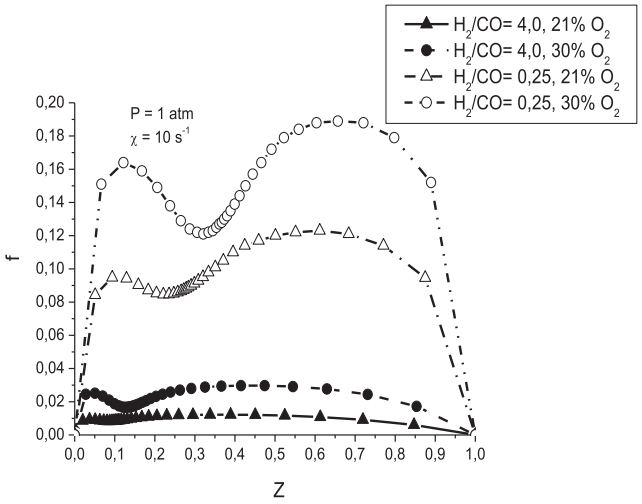

Fig. 7 – Effects of oxygen enrichment on radiation factor (1 atm, 300 K, $\chi = 10\ s^{-1}$).

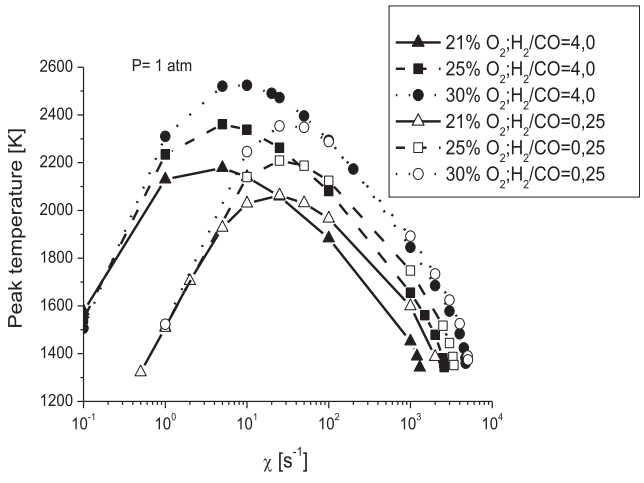

Fig. 8 – Effects of oxygen enrichment on peak flame temperature as a function of scalar dissipation (1 atm, 300 K).

leading to quenching [26]. On other side, the temperature reduction at higher scalar dissipation rates is the result of insufficient gas residence time. It can be observed that blow-off limits are extended with oxygen enrichment, while quenching limits remain the same. For instance, for H_2- lean syngas, extinction occurs for a scalar dissipation equal to 2030 s^{-1} for air and 3402 s^{-1} and 4963 s^{-1} for 25% and 30% oxygen concentrations, respectively. In H_2- rich syngas case, extinction occurs at $\chi = 1296\ s^{-1}$ when oxidizer is air. The blow-off limits for 25% and 30% of oxygen concentrations are 2570 s^{-1} and 4730 s^{-1}, respectively. This behavior clearly demonstrates that oxygen enrichment enhances the stability of the syngas flame. These findings are in good agreement with the results of Yepes and Amell AA [13] and Merlo et al. [41].

The maximum flame temperature exhibits a peak at an intermediate scalar dissipation rate for a given value of oxygen for the syngas compositions considered. For values of scalar dissipation rate lower than the intermediate value, flame structure is influenced by combined effects of adiabatic temperature and radiation heat loss, whereas only adiabatic temperature effect prevails at higher values of strain rate.

For both syngas considered, an increase of the maximum flame temperature with oxygen enrichment is noticed at scalar dissipation rate values lower and higher than the intermediate value. Oxygen addition induces an increase in adiabatic flame temperature. This increase is more important than radiation losses (Fig. 8) at strain rates values lower than the intermediate value [13].

For each oxygen composition, the maximum flame temperatures increase more the syngas is H_2-rich for strain rates values below the intermediate value as radiation decreases with hydrogen addition. The opposite behavior is noticed for strain rate values higher than the intermediate value due to the decrease of adiabatic flame temperature with hydrogen enrichment [26,38,39].

Fig. 9 illustrates the predicted NO profiles for the two syngas at different oxygen concentrations. Inlet temperature is 300 K, ambient pressure is 1 atm and the scalar dissipation rate is taken 10 s^{-1}. It can be observed that NO emissions increase with oxygen and this trend is amplified by hydrogen addition in the fuel (rich syngas). Moreover, the maximum values of NO line up with maximum temperatures. This result is concordant with the study of Shih and Hsu [42].

An analysis of NO production pathways (thermal NO, prompt NO and N_2O path) is provided in Fig. 10. NNH route is not considered in this analysis. Indeed, Shih and Hsu [42] observed that NNH route becomes the dominant route for syngas flames only at very low pressures (near 0.01 atm). The results of Fig. 10 indicate that for H_2-lean syngas, thermal NO represents about 66% of the total NO production while it increases to about 84% for H_2-rich syngas. This signifies that the thermal route, also known as Zeldovich's route, is the dominant mechanism for NO formation. This result is in good agreement with the findings of [42]. In addition, oxygen increment is found to largely increase the thermal NO amount. As a result, the total NO production is substantially increased, despite the smaller amount of initial N_2 available in the oxidizer. This trend was also noticed by Sung and Law [43].

Fig. 11 illustrates NO Emission Index (EINO) as a function of scalar dissipation rate, for different levels of oxygen enrichment. The emission index EINO is a global parameter that has

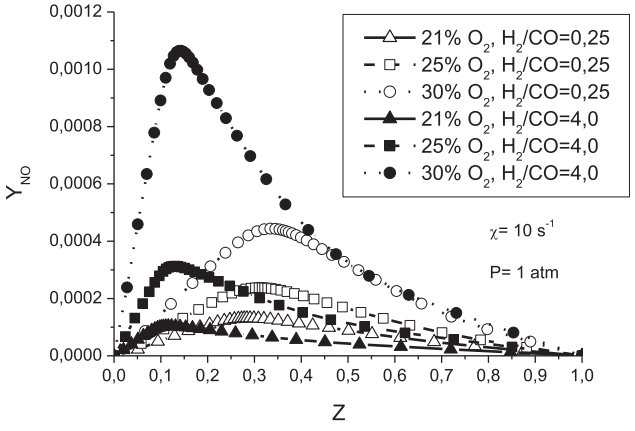

Fig. 9 – Effects of oxygen enrichment on NO emissions (1 atm, 300 K, $\chi = 10\ s^{-1}$).

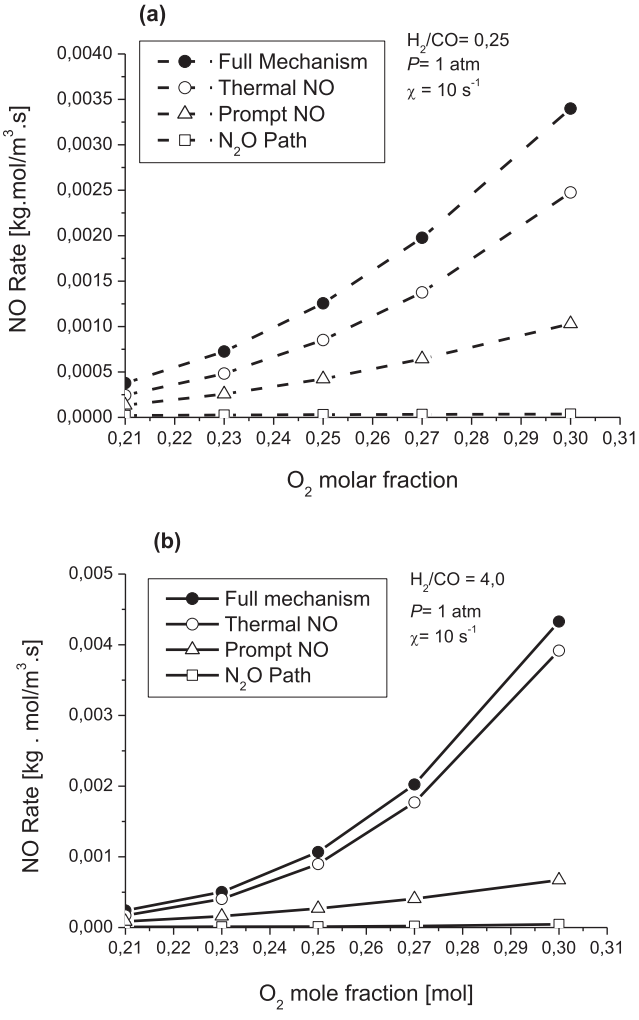

Fig. 10 – NO routes as a function of oxygen concentration for (a) a lean syngas (b) a rich syngas.

been commonly used to characterize NO emission from a flame. It is defined as [44]:

$$EINO = \frac{\int_0^z M_{NO}\dot{\omega}_{NO}dz}{\int_0^z \left(M_{H_2}\omega_{H_2}dz + M_{CO}\omega_{CO}dz\right)} \quad (7)$$

where M represents the molecular weight and $\dot{\omega}$ is the net production/consumption rate. *EINO* exhibits a non-monotonic variation with scalar dissipation rate. It increases to a maximum and then decreases. The peak of *EINO* rises dramatically with oxygen addition and this trend becomes more noticeable for hydrogen-rich syngas. An important observation from these results is the existence of operating conditions that yields lowest amount of NO production. In practice, industrial combustion systems should operate at low scalar dissipations for H_2-lean syngas (about 5 s^{-1}) and high scalar dissipations for H_2-rich syngas (between 100 and 1000 s^{-1}) in order to minimize NO emissions. These findings agree with trends reported in the literature [25].

Conclusions

The present study is a numerical investigation of the effect of oxygen enrichment on the structure and NO_x emissions of a counter-flow syngas flame over a wide range of operating conditions. Oxygen concentrations vary in the range of 21%–30%. Two representative syngas compositions are considered. In addition, this contribution performs an investigation of optimum operating conditions for syngas oxygen enriched combustion in regards to NO_x emissions.

The most important findings are the following:

- Flame thickness decreases with oxygen addition.
- CO_2 production increase with oxygen-enhancement.
- Flame flammability limits are enhanced with oxygen.
- The maximum flame temperature shows a peak at an intermediate scalar dissipation rate for a given value of oxygen for the two syngas compositions considered. For values of scalar dissipation rate lower than the intermediate value, flame structure is influenced by combined effects of adiabatic temperature and radiation heat loss, whereas only adiabatic temperature effect prevails at higher values of strain rate.
- For both syngas considered, an increase of the maximum flame temperature with oxygen enrichment is noticed at scalar dissipation rate values lower and higher than the intermediate value. Oxygen addition provokes an increase in adiabatic flame temperature. This increase is more important than radiation losses at strain rates values lower than the intermediate value.
- For each oxygen composition, the maximum flame temperatures increase more the syngas is H_2-rich for strain rates values below the intermediate value as radiation decreases with hydrogen addition. The opposite behavior is noticed for strain rate values higher than the intermediate value due to the decrease of adiabatic flame temperature with hydrogen enrichment.
- NO emissions dramatically increase with oxygen.
- NO formation is dominated by Zeldovich mechanism.
- Practical burners like gas turbines or boilers should operate at low scalar dissipations for H_2-lean syngas (about 5 s^{-1}) and high scalar dissipations for H_2-rich syngas (between 100 and 1000 s^{-1}) in order to minimize NO_x emissions.

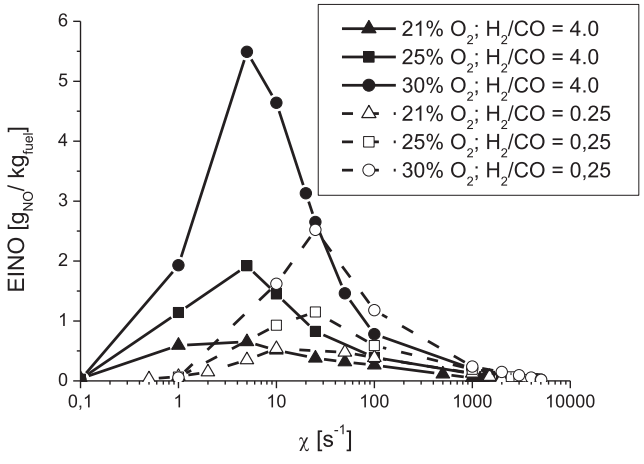

Fig. 11 – NO emission index as a function of scalar dissipation rate, for different levels of oxygen enrichment.

REFERENCES

[1] Gökalp I, Lebas E. Alternative fuels for industrial gas turbines (AFTUR). Appl Therm Eng 2004;24:1655–63.

[2] McLean IC, Smith DB, Taylor CS. The use of carbon monoxide/hydrogen burning velocities to examine the rate of the CO + OH reaction. Symp Int Combust 1994;25:749–57.

[3] Favre E, Bounaceur R, Roizard D. Biogas, membranes and carbon dioxide capture. J Membr Sci 2009;328(1–2):11–4.

[4] Baukal Jr CE. Oxygen- enhanced combustion. Air Products and Chemicals, Inc. 1st ed. Pennsylvania: CRC Press; 1998.

[5] Blasiak W, Yang WH, Narayanan K, Von Schéele J. Flameless oxy-fuel combustion for fuel consumption and nitrogen oxides emissions reduction and productivity increase. J Energy Inst 2007;80:3–11.

[6] D'Agostini M. High-efficiency, high-capacity, low- NO_x aluminum melting, using oxygen-enhanced combustion. Final Report for the U.S Department of Energy. Pennsylvania: Air Products and Chemicals, Inc; may 2000. Cooperative agreement N°. DE-FC07–971D13514.

[7] Tan Y, Douglas MA, Thambimuthu KV. CO_2 capture using oxygen enhanced combustion strategies for natural gas power plants. Fuel 2002;81:1007–16.

[8] Cheng Z, Wehrmeyer JA, Pitz RW. Oxygen-enhanced temperature laminar flames. In: 42nd American Institute of Aeronautics and Astronautics Aerospace Sciences Meeting and Exhibit; 2004 [Reno, Nevada].

[9] Chen R, Axelbaum RL. Scalar dissipation rate at extinction and the effects of oxygen-enriched combustion. Combust Flame 2005;142:62–71.

[10] Urzica D, Gutheil E. Counterflow combustion modeling of CH_4/air and CH_4/O_2 including detailed chemistry. Italy: ILASS; 2008. Sep. 8–10.

[11] Ditaranto M, Oppelt T. Radiative heat flux characteristics of methane flames in oxy-fuel atmospheres. Exp Therm Fluid Sci 2011;35:1343–50.

[12] Joo PH, Charest MRJ, Groth CPT, Gülder OL. Comparison of structures of laminar methane-oxygen and methane- air diffusion flames from atmospheric to 60 atm. Combust Flame 2013;160:1990–8.
[13] Yepes HA, Amell AA. Laminar burning velocity with oxygen-enriched air of syngas produced from biomass gasification. Int J Hydrogen Energy 2013;38:7519–27.
[14] Pitsch H, Peters N. Consistent flamelet formulation for nonpermixed combustion considering differential diffusion effects. Combust Flame 1998;114:26–40.
[15] Peters N. Turbulent combustion. Cambridge University Press; 2000.
[16] Barlow RS, Smith NSA, Chen JY, Bilger RW. Nitric oxide formation in dilute hydrogen jet flames: isolation of the effects of radiation and turbulence- chemistry submodels. Combust Flame 1999;117:4–31.
[17] Frank JH, Barlow RS, Lundquist C. Radiation and nitric oxide formation in turbulent non-premixed jet flames. Proc Combust Inst 2000;28:447–54.
[18] Som S, Ramırez AI, Hagerdorn J, Saveliev A, Aggarwal SK. A numerical and experimental study of counterflow syngas flames at different pressures. Fuel 2008;87:319–34.
[19] Park J, Lee DH, Yoon SH, Vu TM, Yun JH, Keel SI. Effects of Lewis number and preferential diffusion on flame characteristics in 80%H_2/20%CO syngas counterflow diffusion flames diluted with He and Ar. Int J Hydrogen Energy 2009;24:1578–84.
[20] Kim JS, Park J, Kwon OB, Lee EJ, Yun JH, Keel SI. Preferential diffusion effects in opposed-flow diffusion flame with blended fuels of CH_4 and H_2. Int J Hydrogen Energy 2008;33:842–50.
[21] Fluent user's guide ver. 6.2. Fluent Inc.; 2005.
[22] Drake MC, Blint RJ. Structure of laminar opposed-flow diffusion flames with CO/H_2/N_2 fuel. Combust Sci Technol 1988;61:187–224.
[23] Park J, Kwon OB, Yun JH, Keel SI, Cho HC, Kim S. Preferential diffusion effects on flame characteristics in H_2/CO syngas diffusion flames diluted with CO_2. Int J Hydrogen Energy 2008;33:7286–94.
[24] Smith GP, Golden DM, Frenklach M, Moriarty NW, Eiteneer B, Goldenberg et al., GRI MEch-3.0, <http://www.me.berkeley.edu/grimech/.
[25] Park J, Bae DS, Cha MS, Yun JH, Keel SI, Cho HC, et al. Flame characteristics in H_2/CO synthetic gas diffusion flames diluted with CO_2: effects of radiative heat loss and mixture composition. Int J Hydrogen Energy 2008;33:7256–64.
[26] Shih HY, Hsu JR, Lin YH. Computed flammability limits of opposed-jet H_2/CO syngas diffusion flames. Int J Hydrogen Energy 2014;39:3459–68.
[27] Davis SG, Joshi AV, Wang H, Egolfopoulos F. An optimized kinetic model of H_2/CO combustion. Proc Combust Inst 2005;30:1283–92.
[28] Petrova MV, Williams FA. A small detailed chemical–kinetic mechanism for hydrocarbon combustion. Combust Flame 2006;144(3):526–44.
[29] Mueller MA, Yetter RA, Dryer FL. Flow reactor studies and kinetic modeling of the H_2/O_2/NO_x and CO/H_2O/O_2/NO_x reactions. Int J Chem Kinet 1999;31:705–24.
[30] Singh D, Nishiie T, Tanvir S, Qiao L. An experimental and kinetic study of syngas/air combustion at elevated temperatures and the effect of water addition. Fuel 2012;94:448–56.
[31] Sahu AB, Ravikrishna RV. A detailed numerical study of NO_x kinetics in low calorific value H_2/CO syngas flames. Int J Hydrogen Energy 2014;39:17358–70.
[32] Li J, Zhao Z, Kazakov A, Chaos M, Dryer FL, Scireijr JJ. A comprehensive kinetic mechanism for CO, CH_2O, and CH_3OH combustion. Wiley InterScience; 2006.
[33] Ranzi E, Frassoldati A, Faravelli T. The ignition, combustion and flame structure of carbon monoxide/hydrogen mixtures. Note 1: detailed kinetic modeling of syngas combustion also in presence of nitrogen compounds. Int J Hydrogen Energy 2007;32:3471–85.
[34] Cheng Z, Wehrmeyer JA, Pitzhanced RW. Experimental and numerical studies of opposed jet oxygen-enhanced methane diffusion flames. Combust Sci Technol 2006;178:2145–63.
[35] Seshadri K, Puri I, Peters N. Experimental and theoretical investigation of partially premixed diffusion flames at extinction. Combust Flame 1985;61:237–49.
[36] Chan SH, Yin JQ, Shi BJ. Structure and extinction of methane-air flamelet with radiation and detailed chemical kinetic mechanism. Combust Flame 1998;112:445–56.
[37] Shih HY. Computed extinction limits and flame structures of H_2/O_2 counterflow diffusion flames with CO_2 dilution. Int J Hydrogen Energy 2009;34:4005–13.
[38] Safer K, Tabet F, Ouadha A, Safer M, Gökalp I. Combustion characteristics of hydrogen-rich alternative fuels in counter-flow flame configuration. Energy Convers Manag 2013;74:269–78.
[39] Safer K, Tabet F, Ouadha A, Safer M, Gökalp I. Simulation of a syngas counter-flow diffusion flame structure and NO emissions in the pressure range 1-10 atm. Fuel Process Technol 2014;123:149–58.
[40] Wu KK, Chang YC, Chen CH, Chen YD. High-efficiency combustion of natural gas with 21–30% oxygen-enriched air. Fuel 2010;89:2455–62.
[41] Merlo N, Boushaki T, Chauveau C, de Persis S, Pillier L, Sarh B, et al. Experimental study of oxygen enrichment effects on turbulent non-premixed swirling flames. Energy & Fuels 2013;27:6191–7.
[42] Shih HY, Hsu JR. Computed NO_x emission characteristics of opposed-jets syngas diffusion flames. Combust Flame 2012;159(5):1851–63.
[43] Sung CJ, Law CK. Dominant chemistry and physical factors affecting NO formation and control in oxy-fuel burning. Proc Combust Inst 1998;27(1):1411–8.
[44] Giles DE, Som S, Aggarwal SK. A numerical investigation on the structure and emission characteristics of counterflow syngas flames. Fuel 2006;85:1729–42.